Successive Impact of Segmented Rods at High-Velocity

Minhyung Lee* and Michael J. Normandia**

(*Received April 28, 1998*)

The penetration capabilities of segmented rods consisting of multiple, small aspect ratio segments, $(1/8<L/D<1)$ are examined. Our investigation consisted of a series of axisymmetric numerical simulations for constant mass, diameter, and collapsed length. The calculations are limited to tungsten alloy in the form of segmented rods impacting rolled homogeneous armor steel (RHA) at 2.6 km/s successively with infinite spacing. The results of our numerical calculations show that the degradation of penetration performance of successive segments is indeed more pronounced for segments of smaller aspect ratios even at an impact velocity of 2. 6 km/s. There is a continual degradation of performance for $L/D<1$ segments with the amount of degradation increasing as the aspect ratio decreases. The degradation in penetration is attributed to the material remaining in the cavity. This is verified from another set of simulations (the projectile residue was removed before the impact of the successive segments) which shows almost no degradation. There is a shift in the optimal segment size toward increasing segment aspect ratios when multiple segments are considered as compared to when only single segment performance is considered.

Key Words: Segmented Rods, Impact, High Velocity, Penetration, Degradation,

Nomenclature

D	: Segment diameter
D_c	: Cavity diameter
G	: Shear modulus
KE	: Impact kinetic energy
L	: Projectile length
L_t	: Collapsed length
P	: Penetration depth
P_t	: Accumulated penetration depth
V	: Impact velocity
V_c	: Cavity volume
Y	: Yield strength
ε^p	: Equivalent plastic strain
ε^*	: Dimensionless plastic strain rate
ρ_p	: Density of projectile
ρ_t	: Density of target
σ	: Von Mises effective flow stress

* School of Mech. & Aero. Engineering, Sejong University, Korea
** Institute for Advanced Technology
The Univ. of Texas at Austin, USA

1. Introduction

Most of the work examined in the open literature concerned with multiple segment performance was performed using $L/D=1$ segments, while work examined for $L/D<1$ segments was mostly for single segment performance. L and D are the length and diameter of the segments, respectively. The potential improvement in penetration performance per unit collapsed length of single segment is enormous, if it could be realized. Collapsed length is the total length without spac-

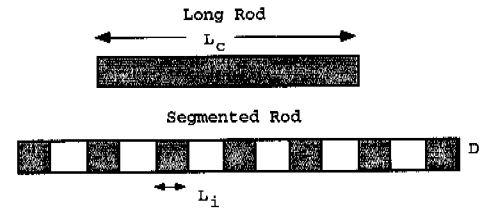

Fig. 1 Definition for long rod and segmented rods, L_c is the collapsed total length, L_i is the segment length and D is the diameter.

ing as shown in Fig. 1. For an impact velocity of 2.6 km/s, Orphal et al.(1993) demonstrate that segments of $L/D=1/8$ are optimal, which is in agreement with Bjerke et al.(1992) who conducted experiments and calculations at 2 km/s. The penetration of segmented rods exhibited large scatter, but $L/D=1/8$ segments demonstrated a performance increase of approximately 87% versus $L/D=1$ segments (P/L of 4.35 vs. 2.4), which themselves are about 65% more effective on a per mass, and per unit collapsed length basis than $L/D\geq 30$ (Herrmann, 1987), long-rod penetrators (P/L of 2.4 vs. 1.45). Thus, overall performance increases of over 300% are possible for $L/D=1/8$ segments as compared to long rods, if they can be realized and engineered.

The increased penetration depth per unit of collapsed length, P/L, is well known and the reader is referred to Kienie et al. (1994) for a historical perspective and for summaries of the work of Hohler and Stilp, Orphal, Bjerke, Zukas. The increase in P/L is achieved at a cost as demonstrated by Orphal (1995) and summarized by Reinecke (1996) who examined the ratio of impact kinetic energy to target crater volume. This ratio increases as the segment aspect ratio is reduced, and quite dramatically for $L/D \geq 1/8$, although this is a function of impact velocity. More specifically, penetration depth is achieved at the expense of penetration diameter. Our calculations at 2.6 km/s show a crater diameter to penetration diameter ratio of 1.6 D for the first $L/D=1/8$ segment, as compared to 2.64 for a $L/D=1$ segment, which is a difference of over 60%. Both values are consistent with the experimental data reported in the literature (Orphal et al., 1995, Hohler and Stilp, 1990).

Many potential factors limit the terminal performance of multiple segmented rods. Other than the engineering issues and associated parasitic mass necessary to launch and deploy the segment train, performance has been demonstrated to be a strong function of segment spacing (Scheffler, 1989, Zukas, 1990, Franzen et al., 1994, Cline et al., 1988), segment alignment and reduced crater diameter (Hohler and Stilp, 1990), and residual projectile material remaining at the bottom of the crater (Hauver and Melani, 1990). Despite all of these challenges and issues, the segmented penetrator performance on a penetration depth criterion is still significantly more effective on a per unit collapsed length, mass, or energy basis.

For $L/D=1$ segmented rods, Hohler and Stilp (1990) conducted experiments at 2.5 km/s and measured only 90% of the penetration depth obtained by multiplying the single segment depth times the number of segments. They attributed performance reduction to impact of the crater wall. One notable attribute was a decreasing crater volume for successive segments. Experiments were also conducted by Frank et al. (1998), at 1.85 km/s in which single $L/D=1$ segment was fired into a rolled homogeneous armor steel (RHA), and after the target was recovered, it was impacted successively so that five segments impacted the same penetration channel. They measured very *little change* in unit penetration depth for all five segments, although the crater diameter was decreasing. In addition, they also fired $L/D=1$ segments into predrilled cylindrical holes of the same depth as the first segment penetration depth within the target in the velocity range between 1.65 km/s and 1.8 km/s. This investigation examined the effect of segment material in the cavity bottom on the performance of the successive segments. The measured penetrations were slightly greater than those measured for single segment impacting on a flat target without predrilled holes.

To examine the weaponization potential of segmented rod performance, De Rosset and Sherrick (1996) reported on CTH numerical simulations for a fixed segment spacing at 1.7 and 2.6 km/s against RHA. They observed that the penetration degradation could be attributed to the successive segments impacting the rear of the previous segments. This effect was more pronounced at low velocities. Hauver and Melani (1990) also found that successive segments contribute progressively less to the total penetration because of their interaction with residue. Since unitary rods of gold-alloy leave almost no residue, they experimented with gold alloy rods. However, the absolute penetration performance of

gold alloy segmented rods was poor relative to tungsten because of its very low strength.

Summarizing the results for $L/D=1$ segments, there appears to be little or no performance degradation (on the order of 10%), although deep segment penetration has not been thoroughly investigated. For $L/D<1$, on the other hand, most of the experiments and calculations were performed for single segment. The work done to investigate the multiple segment performance concentrated on segment spacing and did not thoroughly investigate the consequences of either material remaining at the crater bottom or of entrance effects.

In the present work, the spacing parameter between each segment was eliminated by performing the calculations of successive segments one at a time into the recovered target after the individual segment penetration processes came to a complete stop. Numerical time history data obtained consisted of penetration velocity, depth of penetration and crater diameter. Additional calculations were conducted to investigate the observed penetration degradation for the $L/D=1/8$ and $L/D=1/4$ segments. A calculation of tungsten impacting tungsten was performed as a limiting case of residue accumulation. Additional calculations were also made in which the remaining residue material was removed from the crater bottom before performing the subsequent calculations. This differs from predrilled holes as it retains the unique crater geometry made by each segment. For non-cylindrical cavities, the subsequent segment impacts the crater wall before it reaches the crater bottom.

Where possible, we compared the calculation resalts with other work in the literature and our results agreed well. The calculations show a clear delineation between $L/D=1$ segmented rods and $L/D=1/8$ segmented rods as well as a transitional behavior for $L/D=1/4$ and $1/2$ segmented rods. The results also help to clarify the performance difference between segments of different aspect ratios. Theresidual rod material remaining is the primary factor which degrades the penetration performance. Entrance effects were known to be insignificant for long rods, but deserved further investigation for very short segments. The calculations showed that the entrance effect did not affect the penetration depth, but it did significantly effect the crater diameter.

2. Numerical Simulations

Numerical simulations of tungsten segmented rods ($L/D=1/8$, $1/4$, $1/2$, and 1) impacting semi-infinite RHA steel targets were conducted using the AUTODYN finite-difference code. The conservation equations of mass, momentum, and energy are coupled with specified constitutive laws and equation of state to arrive at a direct numerical solution of the problem. An Eulerian mesh is generated to model both the target and the segmented rods. With an Euler grid, the material flows through a fixed mesh, so there will be no numerical mesh deformation. In this study a two-dimensional axisymmetric calculation was performed. We fixed the diameter of each segment to 16 mm and the impact velocity was fixed at 2.6 km/s. The matrix of computer simulations performed is listed in Table 1.

Two sets of calculations were performed assuming axial symmetry. Initially, for $L/D=1/8$ the target radius was 45 mm, which might be small to simulate the semi-infinite target. We recalculated the whole matrix of numerical simulations with the new meshe representing the target, as shown in Table 1. The grid size was made more uniform and of greater lateral extent. This was based on the work of Partom(1994) who demonstrated

Table 1 Matrix of computer calculations at 2.6km/s and infinite segment spacing

		Target size		Notes
L/D	# of segment	Radius (mm)	Thickness (mm)	
1	1	150	Semi-infinite	
1/2	2	140	Semi-infinite	
1/4	4	130	Semi-infinite	
1/4	4	130	Semi-infinite	Most of tungsten in crater removed
1/8	8	120	Semi-infinite	
1/8	8	120	Semi-infinite	Most of tungsten in crater removed

target strength degradation effects for targets of finite lateral extent. The specific penetration numbers differ from the first set of calculations, but all of the trends observed are identical between the two sets. A transmissive boundary condition was utilized on the rear surface (120 mm) to emulate a semi-infinite thick target.

The Mie-Gruniesen equation of state (E.O.S.) is used for both the projectile and target materials. The parameters are the same as those used by Lee and Bless (1998). We used a constant shear modulus, G (140GPa) and a von-Mises yield surface with a yield strength, Y (2GPa) for tungsten segmented rods. Two levels of failure models are used, both of which are based on the effective plastic strain (Bjerke, 1992). When the first failure level of strain is reached, the element behaves like fluid and can only support hydro-dynamic compression. The element is completely removed from the calculation when the second failure level of strain, set at 250%, is reached. The constitutive response for RHA steel was represented by the Johnson-Cook model:

$$\sigma=[960+1330(\varepsilon^{p})^{0.85}][1+0.06875\ln\varepsilon^{*}][1-T^{*1.15}]\ \text{MPa} \quad (1)$$

where σ is the von Mises effective flow stress, ε^{p} is the equivalent plastic strain, ε^{*} is the dimensionless plastic strain rate, and T^{*} is the homogeneous temperature.

3. Results and Discussions

3.1 Penetration phases

Figure 2 depicts the penetration and tail velocities along the center line as a function of time, for the impact of a single $L/D=1/8$ segment. For the long rods, the tail velocity decreases slowly, however, the small aspect segment, the tail velocity decreases quickly. At this aspect ratio, a condition of steady flow is established after several rarefaction waves have traversed between the rear of the segment and the impact interface, but before the side rarefaction wave arrives at the centerline. For segments with greater aspect ratios, the ratio of the longitudinal to radial wave traversal times increases, becoming approximately

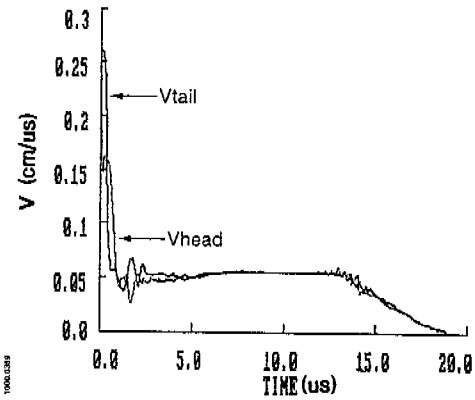

Fig. 2 Penetration and tail velocities for $L/D=1/8$.

equal for $L/D=1/4$ to $1/2$, and much larger for longer segments and for long rods (Bjerke, 1992).

3.2 Segment penetration data

The penetration depth, P, from the calculations was determined by measuring the distance from the undisturbed target surface to the deepest location of the crater bottom at the interface between the segment and target material. Infinite spacing between each segment was modeled by conducting simulations until the penetration velocities of the segment become less than 1% of the impact velocity. Figure 3 shows the normalized penetration, P/L, versus number of successive segments for $L/D=1/8$, $1/4$, $1/2$, and 1 for the impact velocity of 2.6 km/s. Experimental data (Hohler and Stilp, 1990) for $L/D=1$ is also shown in the figure for comparison. The trend of penetration per unit length, P/L as a function of segment L/D for the first segment agrees with that reported in the literature: P/L increases with decreasing L/D over the range $1/8<L/D<1$. The penetration of the second segment is smaller than the first segment in all cases with the possible exception of $L/D=1$, which shows almost no decrease. These calculations are also consistent with the experiments of Frank et al. (1988) which show a nearly constant penetration for each $L/D=1$ segment for up to 5 segments at lower impact velocities. Those experiments resulted in almost no material residue at the cavity bottom which is also evident in our calculations.

For $L/D<1$ segments, the penetration

continued to degrade for each successive segment, with the ratio of penetration of segment i to the penetration of the first segment continuing to decrease. The results in Fig. 3 show degradation for the $L/D=1/4$ and $1/2$ segments as well, but to a lesser degree than the $L/D=1/8$ segments. We will discuss the resalts of the $L/D=1/4$ and $1/2$ segments after further investigation of the reasons for the degradation of the $1/8$ segments. For the $L/D=1/8$ segments, there is a reduction of 25% for the second segment as compared to the first segment, a 26% reduction for the third, a 32% for the fourth and fifth segments. It appeared that this penetration was leveling off.

Each segment impacts a successively larger amount of residual segment material, and after several impacts, the bottom of the cavity will be covered with a significant amount tungsten residue, which the remaining segments must deal with. To estimate the lower bound of P/L for the

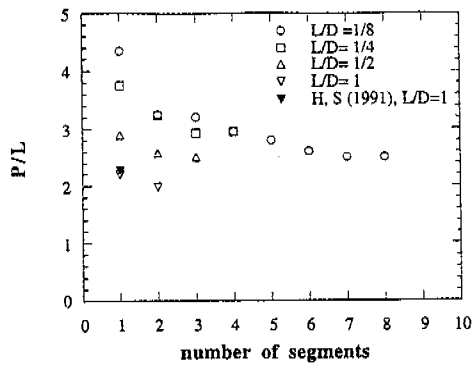

Fig. 3 P/L *vs.* number of segments at 2.6km/s, data by Hohler and Stilp(1991).

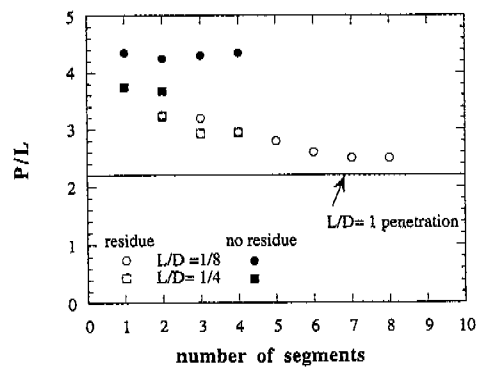

Fig. 4 P/L *vs.* number of segments both with and without residue.

successive $L/D=1/8$ segments, additional calculations were performed. The first of these was that of a single tungsten alloy segment impacting a tungsten alloy target, representative of a continual increase in segment residue at the crater bottom. In this case, the segment P/L is found to be 2.15, considerably lower than the penetration of the eighth segment, suggesting a potential for a further decrease in penetration for the following segments.

Using the $L/D=1/8$ tungsten into steel and tungsten into tungsten first segment penetration values, P/L scales as $(\rho_p/\rho_t)^{0.08}$, where ρ_p and ρ_t are the projectile and target material densities, respectively. Several researchers have estimated that penetration should scale as $(\rho_p/\rho_t)^{1/3}$, $(\rho_p/\rho_t)^{1/2}$ or $(\rho_p/\rho_t)^{2/3}$ for $L/D=1$ projectiles. From the experimental data in the work of Hohler and Stilp(1990), for the case of D17 tungsten alloy impacting German Armor Steel, the value of P/L is 2.276 at 2.602 km/s, and for C110W2 steel impacting German Armor Steel case $P/L=1.141$ at 2.593 km/s. These results for penetration scale as $(\rho_p/\rho_t)^{0.87}$. A more thorough investigation of the scaling exponent is required to explain these trends.

However, it is clear that the consistent degradation in penetration is directly attributed to residual material remaining at the crater bottom. This is based upon an additional set of computations performed specifically for this purpose. In this additional set of calculations, we carefully removed all the residual tungsten from cells at the bottom of the crater, before we resumed the impact of the second segment. Some small amount of tungsten remained along the crater, as attempts to remove it resulted in mixed cells which affected the subsequent calculations. We did this for four successive $L/D=1/8$ segments, and also for two successive $L/D=1/4$ segments. These simulations are actually similar to those with a predrilled hole performed by De Rosset et al. (1996) and Frank et al. (1988) except the shape of the crater was the actual shape. In Fig. 4, the calculated results of the $L/D=1/8$ and $L/D=1/4$ segments are shown both with and without the residual rod material removed. Note that the

penetration is approximately constant when the material is removed, and the penetration performance approaches that of the $L/D=1$ penetration, which showed very little degradation. These results are consistent with those of the predrilled hole test for $L/D=1$ segments (Frank et al., 1988). The calculated value for the fourth $L/D=1/8$ segment is within the expected scatter of the simulations.

From these results we conclude that the penetration degradation of the successive segments is solely due to the segment material remaining in the cavity bottom. These effects become significant for low values of L/D. The performance of segmented rods could be enhanced if somehow the material remaining in the crater bottom can be removed, especially for $L/D<1$.

In Fig. 5, we examine the effectiveness of the various segment aspect ratios by depicting the total penetration (P_t) normalized by the total collapsed segment length (L_t) as a function of the total length normalized by the length of $L/D=1/8$ segment. The results show almost identical penetration for the $L/D=1/8$ and 1/4 segments, up to 8 segments. Clearly, the error in estimating the total penetration depth from that of the first segment penetration and multiplying by the number of segments would continually increase, and the result is worse for small segment size, namely $L/D<1/2$. For L/D 1/2 and $L/D=1$, the error would be minimal.

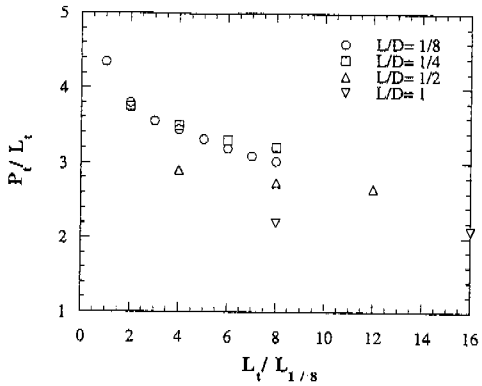

Fig. 5 P_t/L_t *vs.* $L_t/L_{1/8}$ at 2.6km/s.

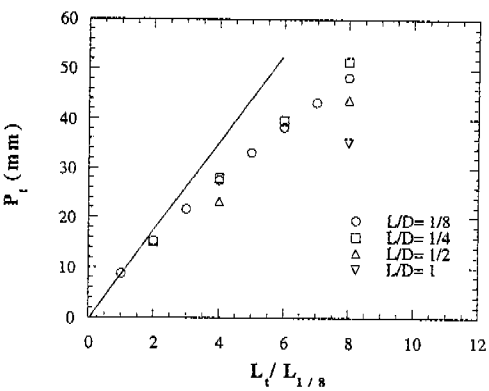

Fig. 6 Total penetration *vs.* normalized total length at 2.6km/s.

In Fig. 6, we show the total penetration versus total collapsed penetrator length, normalized by the length of $L/D=1/8$ segment. For $L/D=1/8$ segments, the total penetration for 8-segmented rods is 48.3 mm, ($P_t/L_t=3.02$) as compared to 69.6 mm using the penetration of the first segment 8.7 mm x 8 segments ($P_t/L_t=4.35$). Thus, the actual penetration performance of a 8-segmented rod consisting of $L/D=1/8$ segments is only 69% of that obtained by the multiplication scheme. Even if the second segment penetration of 6.5 mm was used, the estimated penetration would be 8.7 mm+6.5 mm x 7 segments, or 54.2 mm, still 12% greater than the actual penetration.

Despite this noticeable decrease in penetration, the value of P/L for the eighth segment of $L/D=1/8$ is still 2.5, which is still significantly larger than $P/L=1.45$ for a long-rod ($L/D\geq 30$) at an impact velocity of 2.6 km/s. In addition, compared to an $L/D=1$ segment penetration of 35.2 mm, eight $L/D=1/8$ segments still penetrate 37% more RHA at 2.6 km/s. Our calculations simply suggest that the performance gain of small segments decreases progressively as the number of segments is increased. The absolute gain in penetration is still present and significant.

3.3 Crater diameter

Cavity diameter was also measured at undisturbed target free surface for the first segment and at the largest size for the successive segments. Figure 7 shows the computed normalized crater diameter, D_c/D, versus the number of segments for an impact velocity of 2.6 km/s. The data from the experiments of Hohler and Stilp (1990) is also

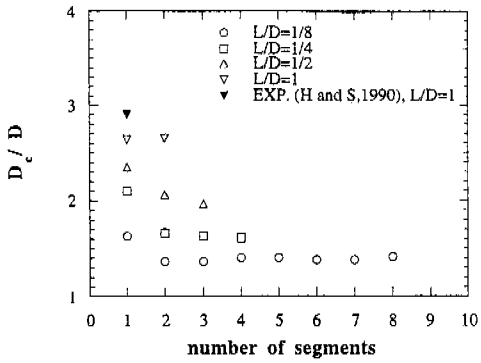

Fig. 7 Normalized crater diameter *vs.* number of segments. Experimental data given by Hohler and Stilp(1990).

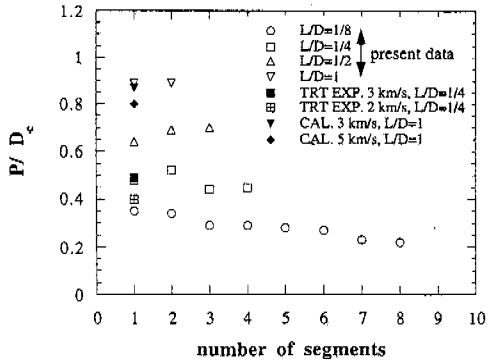

Fig. 8 Penetration depth to crater diameter versus number of segments. TRT denotes the experimental data obtained by Orphal et al., (1993), and CAL denotes the numerical data given by Orphal et al., (1995).

displayed. It is shown that a constant channel shape approaching long-rod behavior is formed from the second segment, with the exception of $L/D=1$. The ratio of the crater diameter to segment diameter decreases with decreasing L/D. A least squares fit of the results of D_c/D versus L/D by linear log-log scale, $D_c/D=(L/D)^s$, gives the following values for s:

Impact velocity (km/s)	s	Correlation coeff.
1.5 (Orphal et al., 1995)	0.14	0.97
2.6	0.225	0.977
3.0 (Orphal et al., 1995)	0.25	0.99

3.4 Crater shape

The ratio of the penetration to crater diameter, P/D_c, is one measure of the crater shape. Figure 8 shows the values of P/D_c versus the number of segments for impact velocity of 2.6 km/s. The experiments performed by Titan Research & Technology are denoted by TRT (Orphal et al., 1993). The computational results given by Orphal et al., (1995) are also displayed. A number of studies have found that for $L/D=1$ cases the crater is not a hemispherical shape, $P/D_c>1/2$. The value $P/D_c=0.88$ calculated here is a little larger than $P/D_c\simeq 0.8$ from Orphal et al. (1995). This is also true for $L/D=1/4$ cases. One possibility of this discrepancy is that the crater diameter is underestimated in the numerical calculations here.

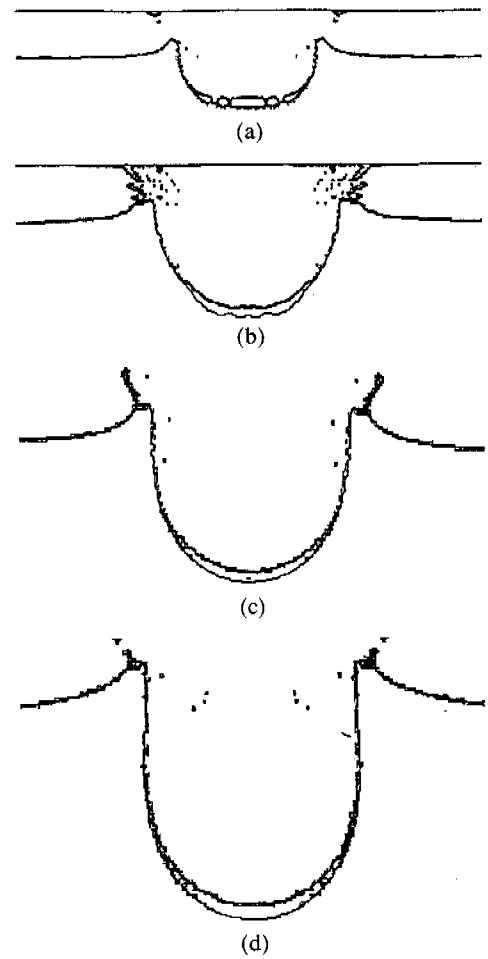

Fig. 9 Craters created by the first segment impacts for $L/D=1/8$(a), 1/4(b), 1/2(c) and 1(d) segments.

For the range of L/D, P/D_c decreases with decreasing projectile L/D. For the successive segmented rods of $L/D=1/8$, the crater shape becomes a shallow disk. This is because the penetration decreases while the crater diameter is the same. Thus, the cratering efficiency (the ratio of impact kinetic energy to crater volume) becomes worse. On the other hand, P/D_c increases for the successive segmented rods of $L/D=1/4$ due to only slight decrease in penetration. To see this trend, the craters generated by the impact of $L/D=1/8$, 1/4, 1/2 and 1 is shown in Fig. 9.

3.5 Crater efficiency (KE/V_c)

It was found by Murphy (1987) that the ratio of impact kinetic energy to crater volume did not vary greatly for a given material. However, it was also found that there is variations of the parameter KE/V_c with segment L/D for $L/D<1$, increasing with decreasing segment L/D (Orphal, et al., 1995). In order to examine this trend of increasing KE/V_c with decreasing L/D, we estimated the actual crater volume from the numerical simulations, although other workers usually measured the crater volume by assuming cylindrical shape. As discussed previously, the crater diameter is largest for the first segment and decreases for successive segments.

In Fig. 10, the estimated values for KE/V_c, including the results given by Orphal et al. (1993) are shown. The present results, within limited data up to $L/D=1/8$, also suggest that KE/V_c increases with decreasing segment L/D, specially for segments with $L/D<1/4$ as discussed by Orphal, et al. (1995). Thus the small L/D projectiles are less effective in terms of crater volume. As shown in the figure, the present results are in the reasonable range compared with other data. Note that TRT data at 5 km/s was carried out twice.

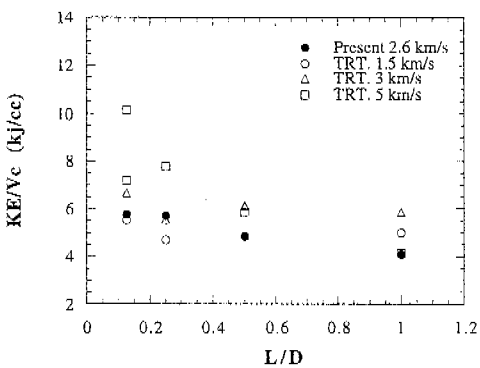

Fig. 10 Kinetic energy per unit crater volume versus L/D.

4. Summary

In the present effort, we performed a successive set of numerical calculations which revealed an increasing amount of degradation as the segment aspect ratio was reduced. This degradation was measured in reduced penetration depth, reduced crater diameter and hence reduced crater volume per unit of penetrator impact energy. Additional calculations were conducted for impacting tungsten targets as a limiting case of a cumulation of residue and the results suggest that further degradation is possible if this limit is actually achieved in deep penetration. However, there is no evidence that this is the case.

A second set of calculations were conducted in which the remaining residue material was removed from the crater bottom before performing the subsequent calculation. These clearly revealed that residual segment material is the primary cause of degradation. Entrance effects did not affect the penetration depth, but did significantly affect the crater diameter. Where possible, our computational results compared favorably with other work in the literature. The calculations showed a clear delineation between $L/D=1$ segments and $L/D=1/8$ segments as well a transitional behavior for $L/D=1/4$ and 1/2 segments.

Despite all of these challenges and issues, the segmented rod performance on a penetration depth criterion is still significantly more effective on a per unit collapsed length, mass, or energy basis. A significant result of this effort suggests that the optimum segment aspect ratio shifts toward higher aspect ratios for multiple segments and may shift further still for very deep penetration. Our investigation thus far has been limited

to normal impacts. The effects of misaligned impacts will be investigated.

Acknowledgments

This work was supported by the U. S. Army Research Laboratory (ARL) under contract DAAA21-93-C-0101.

References

Bjerke, T. W., Zukas, J. A. and Kimsey, K. D., 1992, "Penetration Performance of Disk Shaped Penetrators," *Int. J. Impact Engng*., Vol. 12, No. 2, pp. 263~280.

Cline, C. F., Gogolewski, R. P., Reaugh, J. E., Kubusov, A. S., Ford, B. L., Anderson, G. D. and Holt, A. C., 1988, Final Report for the DARPA Impact Physics Program: Physics of High-Velocity Penetration, LLNL Report, UCID-21728, Livermore, CA, November.

De Rosset, W. S. and Sherrick, T., 1996, "Segmented Rod Performance at Ordance Velocity," ARL-MR-291, Army Research Lab, Aberdeen Proving Ground, MD, Feburary.

Frank, K. L., Zook, J., Spangler, J. and Keele, M., 1988, "Experiments with High Density Segmented Penetrator Element," Army Research Lab, Aberdeen Proving Ground, MD, May.

Franzen, R. R., Walker, J. D., Orphal, D. L. and Anderson, C. E., 1994, "An Upper Limit for the Penetration Performance of Segmented Rods with Segment-$l/d \leq 1$, *Int. J. Impact Engng*., Vol. 15, No. 5, pp. 661~668.

Hauver, E. and Melani, A., 1990, "Behavior of Segmented Rods During Penetration," BRL-TR-3129, Ballistic Research Lab, Aberdeen Proving Ground, MD. July.

Herrmann, W. and Wilbeck, J. S., 1987, "Review of Hypervelocity Penetration Theories," *Int. J. Impact Engng*., Vol. 5, pp. 307~322.

Hohler, V. and Stilp, A., 1990, "Penetration Performance of Segmented Rods at Different Spacing: Comparison with Homogeneous Rods at 2.5-3.5 km/s," Proc. of the 12th Int. Ballistic Sym, San Antonio, USA.

Kiehne, T. M., Orphal, D. L., Normandia, M. J., Bless, S. J. and Stroebel, E., 1994, Review of Research on Segmented Rods, Focusing on DARPA Efforts, IAT R.0062, November.

Lee, M. and Bless, S. J., 1998, "Cavity Dynamics for Long-Rod Penetration," *Int. J. Impact Engng*. Vol. 21 (10), pp. 881~894.

Murphy, M. J., 1987, "Survey of the Influence of Velocity and Material on the Projectile Energy/Target Hole Volume Relationship," 10th Int. Ballistic Sym. San Diego, CA.

Orphal, D. L., Anderson, C. E., Franzen, R. R., Walker, J. D., Schneidewind, P. N. and Majerus, M. E., 1993, "Impact and Penetration by $L/D<1$ Projectiles," *Int. J. Impact Engng*., Vol. 14, pp. 551~560.

Orphal, D. L., Franzen, R. R., Babcock, S. M. and Snedeker, R. S., 1993, "Experimental Measurements of Penetration by $L/D<1$ Projectiles," CRT-TR-3294-14, California Research & Technology, Titan Corporation, C. A.

Orphal, D. L., Anderson, C. E., Franzen, R. R. and Babcock, S. M., 1995, "Variation of Crater Geometry with Projectile L/D for $L/D \leq 1$," *Int. J. Impact Engng*., Vol. 17, No. 2, pp. 595~604.

Partom, Y. and Littlefield, D. L., 1994, "Validation and Calibration of a Lateral Confinement Model for Long Rod Penetration at Ordinance and High Velocities," *Int. J. Impact Engng*., Vol. 17.

Reinecke, W. R., 1996, "A Comparison of RHA Penetration and Critical Angle of Attack Among Monolithic, Segmenting, and Extending Tungsten Rods at 2.5 km/s," IAT TM, July.

Scheffler, D. R., 1989, "Two-Dimensional Computer Simulations of Segmented Penetrators," Report No. BRL-TR-3013, Army Ballistic Research Lab, Aberdeen Proving Ground, MD, July.

Zukas, J. A., 1990, "Numerical Simulation of Semi-Infinite arget Penetration by Continuous and Segmented Rods, Report No. BRL-TR-3081, Army Ballistic Research Lab, Aberdeen Proving Ground, MD, February.